Institut für Numerische Simulation
Rheinische Friedrich-Wilhelms-Universität Bonn

Wegelerstraße 6. 53115 Bonn. Germany
phone +49 228 73-3427. fax +49 228 73-7527
www.ins.uni-bonn.de

Maharavo Randrianarivony

Hierarchical a-posteriori estimator + Nonlinear Poisson-Boltzmann

INS Preprint No. ****

November 2013

HIERARCHICAL A-POSTERIORI ESTIMATOR + NONLINEAR POISSON-BOLTZMANN

MAHARAVO RANDRIANARIVONY

Abstract. We consider the Poisson-Boltzmann problem for the ionic interaction between solute and solvent media. We emphasize on the nonlinear form of the equation without using a linearization. We consider a-posteriori error estimates which can be computed very efficiently. Although the initial problem is a nonlinear one, the error estimator is a linear one. To corroborate the analysis, we report on a few numerical results for illustrations. We compute numerically the values of the constants seen from the theoretical study. A brief survey of the solving of the nonlinear system resulting from the FEM discretization is reported.

1. Introduction

We encounter the nonlinear Poisson-Boltzmann Equation in different areas including: plasma physics, ionic solution, highly charged macroparticles, FET and MOSFET. We consider here the PBE for the interaction of solute and solvent media which are respectively denoted by $\mathbf{\Omega^u}$, $\mathbf{\Omega^v}$ as in in Fig. 1(a). The surface $\mathbf{\Gamma}$ represents the solute-solvent boundary which is in our case the molecular surface as in Fig. 1(b). The solvent is represented by a continuous dielectric medium while the solute is located inside the cavity $\mathbf{\Gamma}$. In the sequel, the whole solute-solvent domain is denoted by $\mathbf{\Omega} := \mathbf{\Omega^u} \cup \mathbf{\Omega^v}$. In this document, we consider the nonlinear PBE whose general expression with the

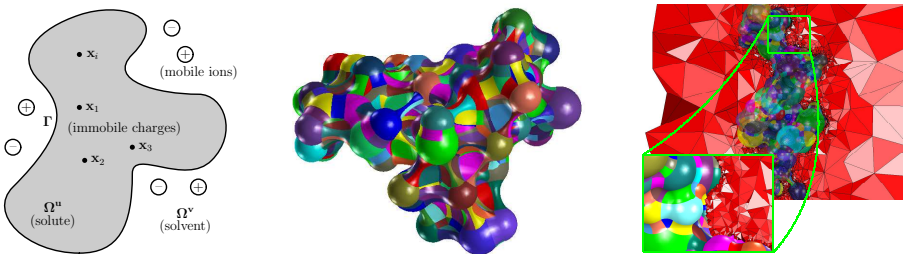

(a) (b) (c)

Figure 1. (a)Solute/solvent regions, (b)Molecular surface, (c)Mesh around the molecule.

unknown function u is

$$-\nabla\cdot(\varepsilon(\mathbf{x})\nabla u(\mathbf{x}))+\sum_{i=1}^{M} n_i q_i \kappa(\mathbf{x}) e^{-\beta q_i u(\mathbf{x})} = \frac{4\pi e_C^2}{k_B T}\sum_{i=1}^{N_m} z_i \delta(\mathbf{x}-\mathbf{x}_i) \qquad \forall\, \mathbf{x}\in\boldsymbol{\Omega}, \tag{1.1}$$

such that $u(\mathbf{x}) = g(\mathbf{x})$ for all $\mathbf{x}\in\partial\boldsymbol{\Omega}$. The coordinates $\mathbf{x}_i$ are the atom centers located in the interior of the molecular region $\boldsymbol{\Omega}^{\mathbf{u}}$. The parameters n_i, k_B, T, e_C, β are physical quantities. The unknown function is the dimensionless electrostatic potential u is related to the electrostatic potential Φ by

$$u(\mathbf{x}) = \frac{e_C\Phi(\mathbf{x})}{k_B T}. \tag{1.2}$$

The coefficients $\varepsilon(\mathbf{x})$ and $\kappa(\mathbf{x})$ are in general space-dependent functions but we consider only the situation where $\varepsilon(\mathbf{x}) := \varepsilon_{\mathbf{u}}$ for $\mathbf{x}\in\boldsymbol{\Omega}^{\mathbf{u}}$ and $\varepsilon(\mathbf{x}) := \varepsilon_{\mathbf{v}}$ for $\mathbf{x}\in\boldsymbol{\Omega}^{\mathbf{v}}$ while $\kappa(\mathbf{x}) := \kappa_{\mathbf{u}}$ for $\mathbf{x}\in\boldsymbol{\Omega}^{\mathbf{u}}$ and $\kappa(\mathbf{x}) := \kappa_{\mathbf{v}}$ for $\mathbf{x}\in\boldsymbol{\Omega}^{\mathbf{v}}$. Those coefficients are discontinuous between $\boldsymbol{\Omega}^{\mathbf{u}}$ and $\boldsymbol{\Omega}^{\mathbf{v}}$ but the solution u is required to be continuous everywhere. We follow the method of Chen and Holst [1] by treating the PBE with FEM (Finite Element Method). Most methods [2, 3] based exclusively on BEM (Boundary Element Methods) consider only the linearized PBE because it is difficult to use fundamental solutions for nonlinear PBE. Although the method can be extended to the general case, we will restrict ourselves to the monovalent case $M = 2$ where the nonlinear term of (1.1) becomes $\sum_{i=1}^{M} n_i q_i \kappa(\mathbf{x}) e^{-\beta q_i u(\mathbf{x})} = \kappa(\mathbf{x})\sinh[u(x)]$. In addition, the right hand side is replaced by a general function $f(\mathbf{x})$ in order to compare the error between the exact solution with the computed one. We develop here a-posteriori estimates based on space enrichment. Such an estimator is also used in [4] but not in the context of nonlinear Poisson-Boltzmann as presented here. Our former investigations are as follows. We have applied mesh generation on molecular surfaces such as in Fig.1(c). The FEM implementation for linearized PBE on parallel machines is detailed in [5]. Mesh generation on parallel processors is under development where the coarsest mesh is not loaded in one processor. The a-posteriori estimator presented here is a generalization of the method in [6]. Treatments of molecular data are published in our previous works [7, 2, 3].

2. Space enrichment for nonlinear Poisson-Boltzmann

Let us present in this section an a-posteriori error estimator base on space enrichment. It is beyond the scope of this short paper to present detailed proof. The following results apply for the general case but we use only the piecewise linear setting in the 2D case because of scarcity of space. The exact solution u belongs to $\mathbf{V} := \mathbf{H}^m(\boldsymbol{\Omega})$ for m sufficiently large. Suppose u_h is the current FEM solution from the piecewise linear

Key words and phrases. Poisson-Boltzmann, A-posteriori error estimator.

space $\mathbf{V}_h$ on a mesh $\mathbf{M}_h$. We want to estimate the error inside an arbitrary triangle T of $\mathbf{M}_h$. Let ε_T and κ_T represent the restriction of the piecewise constant functions $\varepsilon(\mathbf{x})$ and $\kappa(\mathbf{x})$ on T. Denote by a_1, a_2, a_3 the midpoints of its edges and by ϕ_i, $i = 1, 2, 3$ the linear polynomials in T for which $\phi_i(a_j) = \delta_{ij} \quad i, j = 1, 2, 3$. We uniformly refine T into 9 similar triangles and denote by $b_1, ..., b_7$ the nodes which do not coincide with the apices of T. Finally, let ψ_j be the piecewise linear nodal basis functions at b_j. The spaces spanned by ϕ_i and ψ_j are denoted by $\mathbf{V}(T)$ and $\mathbf{W}(T)$ respectively. Denote

$$\langle u, v\rangle_{1,T} := \int_T \nabla u \cdot \nabla v \qquad \text{and} \qquad |u|_{1,T} := \langle u, u\rangle_{1,T}^{1/2}. \tag{2.3}$$

$$\langle u, v\rangle_{0,T} := \int_T u \cdot v \qquad \text{and} \qquad |u|_{0,T} := \langle u, u\rangle_{0,T}^{1/2}. \tag{2.4}$$

There are two constants $\gamma_1, \gamma_2 \in [0, 1)$ which are independent of the geometric properties of T such as the largest edge length $h(T)$, the aspect ratio $\rho(T)$ and the area $\mu(T)$ such that

$$\langle u, v\rangle_{1,T} \leq \gamma_1 |u|_{1,T}.|v|_{1,T} \qquad \forall u \in \mathbf{V}(T), \quad \forall v \in \mathbf{W}(T), \tag{2.5}$$

$$\langle u, v\rangle_{0,T} \leq \gamma_2 |u|_{0,T}.|v|_{0,T} \qquad \forall u \in \mathbf{V}(T), \quad \forall v \in \mathbf{W}(T). \tag{2.6}$$

Those constants describe the strengthened Cauchy-Schwarz inequality which is numerically used in [6].

$$\mathbf{W}_h := \{v \in L^2(\mathbf{\Omega}) : \quad v|_T \in \mathbf{W}(T) \quad \forall\, T \in \mathbf{M}_h\}. \tag{2.7}$$

Now we enlarge the space $\mathbf{V}_h$ hierarchically into $\widetilde{\mathbf{V}}_h$ by using the direct sum

$$\widetilde{\mathbf{V}}_h := \mathbf{V}_h \oplus \mathbf{W}_h\,. \tag{2.8}$$

For the next discussion, we will use

(2.9)

$$\mathbf{A}(u, v) := \int_{\mathbf{\Omega}} \varepsilon(\mathbf{x}) \nabla u(\mathbf{x}) \cdot \nabla v(\mathbf{x}) d\mathbf{x}, \qquad |\!|\!| u |\!|\!| := \int_{\mathbf{\Omega}} \nabla u(\mathbf{x}) \cdot \nabla u(\mathbf{x}) d\mathbf{x}, \qquad \|u\| := \int_{\mathbf{\Omega}} |u(\mathbf{x})|^2 d\mathbf{x}.$$

Consider the continuous problem of finding $E \in \mathbf{V}$ such that for all $v \in \mathbf{V}$,

$$\mathbf{A}(E, v) + \big\langle \kappa \cosh(u_h) E, v\big\rangle = \langle f, v\rangle - \mathbf{A}(u_h, v) - \big\langle \boldsymbol{\kappa} \sinh(u_h), v\big\rangle. \tag{2.10}$$

One can show that $\|E\|_*$ and $\|u - u_h\|_*$ are equivalent up to some mesh independent factors in which we use $\|\cdot\|_* := |\!|\!|\cdot|\!|\!| + \|\cdot\|$. The function E cannot yet be used as an a-posteriori error estimator because it is in an infinite dimensional space and it cannot be computed element-wise. Find $v_h \in \mathbf{V}_h$ such that for all $v \in \mathbf{V}_h$,

$$\mathbf{A}(v_h, v) + \big\langle \kappa \cosh(u_h) v_h, v\big\rangle = \langle f, v\rangle - \mathbf{A}(u_h, v) - \big\langle \kappa \sinh(u_h), v\big\rangle. \tag{2.11}$$

Find $w_h \in \mathbf{W}_h$ such that for all $v \in \mathbf{W}_h$,

$$\mathbf{A}(w_h, v) + \big\langle \kappa \cosh(u_h) w_h, v\big\rangle = \langle f, v\rangle - \mathbf{A}(u_h, v) - \big\langle \kappa \sinh(u_h), v\big\rangle. \tag{2.12}$$

The following property called saturation assumption:

$$\exists\, \beta < 1 : \quad \|E - w_h\|_* \leq \beta \|E - v_h\|_* \tag{2.13}$$

quantifies that the solution in the larger space $\mathbf{W}_h$ corresponding to the 9 times uniformly refined mesh is more accurate than the solution in the smaller space $\mathbf{V}_h$.

The computation of the a-posteriori error estimator is performed as follows. For each element $T \in \mathbf{M}_h$, let $e_T \in \mathbf{W}(T)$ be the solution to the local problem:

$$\varepsilon_T\, a_T(e_T, v) + \kappa_T \left\langle \cosh(u_T) e_T, v \right\rangle_T = \langle f, v\rangle_T - \varepsilon_T\, a_T(u_T, v) - \kappa_T \left\langle \sinh(u_T), v \right\rangle_T \qquad \forall\, v \in \mathbf{W}(T). \tag{2.14}$$

Under the hypothesis of the saturation assumption (2.13), there exist two constants c_1 and c_2 which are independent of $h(T)$, $\rho(T)$, $\mu(T)$ for all elements T of $\mathbf{M}_h$ such that

$$c_1 \sum_{T \in \mathbf{M}_h} \eta_T^2 \leq |\!|\!| u - u_h |\!|\!|^2 + \|u - u_h\|^2 \leq c_2 \sum_{T \in \mathbf{M}_h} \eta_T^2 \tag{2.15}$$

where

$$\eta_T := \sqrt{|e_T|_{1,T}^2 + |e_T|_{0,T}^2} \qquad \text{or} \qquad \eta_T := \sqrt{\sum_{i=1}^{n_W} a_i (e_T)^2}. \tag{2.16}$$

From (2.10) and the residual, we obtain for all $v \in \mathbf{V}$ that

$$\mathbf{A}(E, v) + \langle \kappa \cosh(u_h) E, v\rangle = \mathbf{A}(u - u_h, v) + \langle \kappa \sinh(u) - \kappa \sinh(u_h), v\rangle. \tag{2.17}$$

Due to the mean value theorem, we deduce for all $v \in \mathbf{V}$

$$\mathbf{A}(E, v) + \langle \kappa \cosh(u_h) E, v\rangle = \mathbf{A}(u - u_h, v) + \langle \kappa \cosh(\theta_h)(u - u_h), v\rangle. \tag{2.18}$$

By using $v := u - u_h$ and the fact that $\cosh\Big[\theta_h(\mathbf{x})\Big] \geq 1$, we obtain

$$|\!|\!| u - u_h |\!|\!|^2 + \|u - u_h\|^2 \leq \mathbf{A}(E, u - u_h) + \langle \kappa \cosh(u_h) E, u - u_h\rangle. \tag{2.19}$$

By using the above facts, one deduces the efficiency and reliability of the a-posteriori estimator.

3. Practical results

The previous strengthened Cauchy-Schwarz are given by

$$\gamma = \sup_{u \in \mathbf{V}(T)} \sup_{v \in \mathbf{W}(T)} \frac{\langle u, v\rangle_T}{|u|_T |v|_T} = \sup_{\underline{u} \in \mathbf{R}^3} \sup_{\underline{v} \in \mathbf{R}^7} \frac{\underline{u}^T B \underline{v}}{(\underline{u}^T A \underline{u})^{1/2} (\underline{v}^T C \underline{v})^{1/2}} \tag{3.20}$$

where we use the stiffness or the mass matrix corresponding to $(\phi_1, \phi_2, \phi_3, \psi_1, ..., \psi_7)$, which has a block structure

$$S = \begin{bmatrix} A & B \\ B^T & C \end{bmatrix}. \tag{3.21}$$

Degree of freedom	Nb. iterat.	Residual	Setup time	Solving time
463,249	129	9.616e-09	0.5228 sec	25.0889 sec
1,547,641	188	9.987e-09	0.8954 sec	42.1407 sec
3,597,985	301	9.070e-09	1.4088 sec	68.5293 sec
7,106,761	320	9.829e-09	2.5147 sec	102.7691 sec
12,080,449	450	9.786e-09	3.9483 sec	186.1989 sec
28,560,961	602	9.500e-09	8.3579 sec	415.1201 sec
41,221,225	572	9.653e-09	10.3053 sec	467.0384 sec

TABLE 3.1. Linear solver using 30 processors to drop the residual error below 1.0e-8. $(\varepsilon_u, \varepsilon_v, \kappa_u, \kappa_v) = (1, 100, 2, 40)$ for piecewise linear.

Therefore, γ is given by the square root of the largest eigenvalue of the generalized eigenproblem

$$(BC^{-1}B^T)\underline{v} = \lambda A\underline{v} \ . \tag{3.22}$$

Suppose the triangle $T \in \mathbf{M}_h$ has the angles (α, β, θ). In the case of the stiffness matrix, it is possible [6] to express the eigenvalues in terms of the angles α and β (we get rid of $\theta = \pi - \alpha - \beta$). It can be shown that one eigenvalue is always zero while the other two eigenvalues are bivariate functions away from the unity. The plots of the two eigenvalues are shown graphically in Fig. 2(a) and Fig. 2(b) in terms of the angles (α, β). One can clearly observe that the two eigenvalues do not attain the unity. As for the FEM-error, the reduction of the error compared to the exact solution has been measured by using the H_1-norm. In Fig. 2(c), one observes a plot of the H_1-error in term of the edge length h. It displays the linear decrease of the energy norm in term of the edge length h which is in full accordance with the theoretical expectation. We consider in fact two simulations where we use the parameters $(\varepsilon_u, \varepsilon_v, \kappa_u, \kappa_v) = (2, 5, 7, 3)$ and $(\varepsilon_u, \varepsilon_v, \kappa_u, \kappa_v) = (1, 20, 20, 3)$. For both cases, one observe the same numerical behavior. The a-posteriori error estimates are equally shown in the same figure. It is observed that when the H_1-error is large, the a-posteriori error is also comparatively large and they decrease proportionally.

The solver of the nonlinear system resulting from the FEM discretization is performed by a combination of Fletcher-Reeves nonlinear CG and a damped Newton using monotony tests. In general, only a few iterations of nonlinear CG and damped Newton are required. In addition, the involved Jacobians are sparse. As a consequence, the main issue is the fast solving of the linear system which occurs in each CG/Newton loop. For that matter, we use the linear solvers with least-square preconditioner using Parasails. The performance of the linear solver is presented in Tab.3.1 for the case $(\varepsilon_u, \varepsilon_v, \kappa_u, \kappa_v) = (1, 100, 2, 40)$. A detail of such a computation on parallel processor is

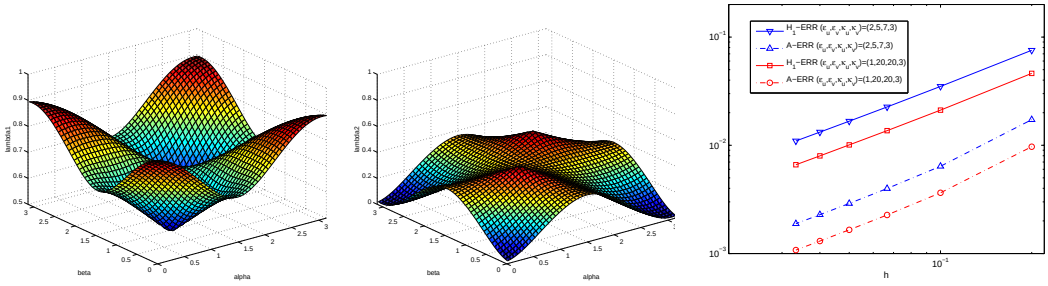

(a) (b) (c)

FIGURE 2. (a)First eigenvalue w.r.t (α, β) (b) Second eigenvalue (c)H_1 and a-posteriori errors.

presented in [5]. As shown in the table, only very few iterations are needed to drop the residual errors very significantly. Both the setup times and the solving times are very fast in comparison to the degree of freedom.

REFERENCES

[1] L. Chen, M. Holst, and J. Xu, *SIAM J. Numer. Anal.* **45**, 2298–2320 (2007).
[2] H. Harbrecht, and M. Randrianarivony, *Computing* **86**, 1–22 (2009).
[3] H. Harbrecht, and M. Randrianarivony, *Computing* **92**, 335–364 (2011).
[4] R. Bank, *Acta Numerica* pp. 1–43 (1996).
[5] M. Randrianarivony, *Parallel Processing of Analytical Poisson-Boltzmann using Higher Order FEM,* in *Proc. Parallel and Distributed Computing and Networks*, 455434, Acta Press, 2013, pp. 1–6.
[6] M. Randrianarivony, *J. Comput. and Appl. Math.* **169**, 255–275 (2004).
[7] M. Randrianarivony, and G. Brunnett, *Lecture Notes in Computational Science and Engineering* **65**, 231–245 (2008).

MAHARAVO RANDRIANARIVONY, VIRTUAL MATERIAL DESIGN, FRAUNHOFER INSTITUTE SCAI, SCHLOSS BIRLINGHOVEN, SANKT AUGUSTIN 53754, GERMANY.

E-mail address: randrian@ins.uni-bonn.de